For. Sci. 65(2):211–222
doi:10.1093/forsci/fxy050

forest management

A Technique for Implementing Group Selection Treatments with Multiple Objectives Using an Airborne Lidar-Derived Stem Map in a Heuristic Environment

Brian M. Wing, Kevin Boston, and Martin W. Ritchie

Group-selection silviculture has many beneficial attributes and has increased in application over the past 30 years. One difficulty with group-selection implementation is the designation of group openings within a stand to achieve a variety of complex management goals. This study presents a new method for utilizing geospatial census stem map data derived from airborne lidar in a heuristic environment to generate and select from treatment solutions that best meet management objectives in an efficient manner. The method successfully generated candidate treatment solutions over two entries that met a set of tree size, opening size and spacing constraints. The heuristic was implemented on two separate ponderosa pine stands with similar stand conditions using different group-selection opening sizes. Successful field implementations relied on a tree-marking technique developed in this study that relied on high-precision GPS receivers. The heuristic identified good solutions, but the quality is unknown as this is a large nonlinear optimization problem. Nonetheless, this study provides an innovative, efficient and mathematically defendable alternative for implementing group-selection treatments in stands where accurate geospatially-referenced census can be obtained.

Keywords: group selection, heuristic, airborne lidar, individual tree detection, census stem map

The use of group-selection silviculture has gained in popularity over the past four decades due to many of its beneficial attributes. A group-selection silviculture method involves removal of small patches of trees that typically create small openings 0.3–0.8 hectares in size mimicking small-scale disturbances caused by natural agents, such as fire, insects, and disease (McDonald et al. 2009). Over time, a shifting mosaic of small tree patches develops across the management unit in multiple age cohorts. The method provides a more aesthetically pleasing alternative to even-aged management because it provides continuous forest cover while retaining productivity and providing additional ecological benefits (Fiske et al. 1992).

In the mixed-conifer and eastside ponderosa pine forests of the Sierra Nevada in California, group-selection silviculture has been used to convert homogeneous stand structures and age classes into more heterogeneous arrangements (McDonald and Abbot 1994, Weatherspoon and Skinner 1996), to maintain or promote late-seral species richness (Shlisky et al. 1999), promote tree regeneration (Stephens et al. 1999), maintain and enhance species diversity and wildlife habitat (Lahde et al. 1999, Schultz 1999), and reduce fire behavior (Moghaddas et al. 2010), and as a means for ecological restoration (Storer et al. 2001). An additional benefit of group-selection silviculture is its implementation flexibility; a variety of specific management objectives can be obtained by varying the size, shape, densities, and layout of the openings. Although having this flexibility is beneficial, it also often creates a complex and challenging decision environment in regard to identifying the best implementation strategies to meet an array of complex management objectives (e.g., stand structure, species composition, harvest volume consistency, wildlife habitat, and fuels reduction). This has

Manuscript received September 28, 2017; accepted October 3, 2018; published online November 15, 2018.

Affiliations: *Brian M. Wing, Deceased, USDA Forest Service Pacific Southwest Research Station, Redding, CA. Kevin Boston (kevinboston@hotmail.com), Department of Forestry and Wildland Sciences, Humboldt State University, Arcata, CA. Martin W. Ritchie (mritchie@fs.fed.us), USDA Forest Service Pacific Southwest Research Station, Redding, CA.*

Acknowledgments: *We would like to thank the USDA Forest Service, Lassen National Forest, Eagle Lake District for helping with implementation of this BMEF study. This study was partially funded by an agreement with USDA Forest Service, Region 5. This manuscript was drafted by Dr. Brian Wing before his untimely death and submitted posthumously.*

caused many forest managers to hesitate or refrain from using the method or exploiting its full potential.

Implementation of group-selection treatments first requires determination of the group size(s) that will be used. Typically, this decision is based on forest type and ecology, site conditions, and management goals (e.g., regeneration, harvest volume, species composition, forest structure, wildlife habitat, fire behavior, large tree retention, etc.). In Sierra Nevada mixed-conifer and eastside ponderosa pine forests, forest managers usually use group-selection treatment sizes ranging from 0.1 to 0.8 hectares (Fiske et al. 1992, McDonald and Abbot 1994, Coates 2000, York et al. 2003). After group size(s) are decided, the number of and spacing between the groups is determined. The number of groups is typically based on the length of time needed to grow mature trees and the planned interval between treatments. For example, if the management goal is to allow 120 years to produce mature trees, and the planned interval between group-selection treatments is 20 years, about one-sixth of the stand area would be removed in each entry. Some form of spacing is then used to ensure the groups are more evenly distributed across a stand to meet management goals. After defining group sizes, treatment periodicity, and group spacing, the layout of the groups is completed using geospatial data and fieldwork.

The goal of group-selection layout is to locate the groups in a manner that achieves specific management goals. These management goals combine interdependent relationships that vary temporally and spatially (e.g., wildlife habitat, timber production, fire and fuels reduction, etc.). This makes implementation of the group-selection layout design very challenging integrating forest inventory and site information that originates from reconnaissance and geospatial-derived data. These data summarize stand and site conditions within a treatment unit at coarse spatial scales. Unfortunately, data at these spatial scales often do not provide the level of detail needed to properly assess the fine-scale heterogeneity within a unit. In addition, the large sampling errors associated with forest inventory data because of low sampling intensity often limit its utility in the layout process. Thus, it is difficult to develop group-selection layout designs that meet multiple management goals in an efficient manner. In the end, the location of the group-selection treatments within a unit is developed from the data available and then implemented on the ground. During implementation, field-based decisions are made that commonly alter the original layout design to adjust to local discoveries made in the field (e.g., individual tree size and characteristics, local tree density and structure, etc.). The combination of these subjective layout design and implementation decisions, proceeding from inadequate information, results in treatment solutions that are fraught with uncertainty.

If higher levels of detail (e.g., census stem map) were available for a treatment unit, it might become possible to develop group-selection treatment solutions in a heuristic environment that provide an opportunity for better solutions to achieve the defined management goals. These solutions would be more defendable in theory, since they would originate from a mathematically driven simulation process that searches a large portion of solution space to identify solutions that better meet the management goals.

Heuristics are increasingly being used to help solve many difficult forest planning problems that are large in size, nonlinear in structure, and spatial in nature (Bettinger et al. 1997, Bettinger et al. 1999, Boston and Sessions 2006, Tóth and McDill 2008). Most forest-planning heuristics have focused on harvest scheduling, wildlife habitat management, and achievement of biodiversity goals. Boston and Sessions (2006), and Tóth and McDill (2008) developed heuristics that included the ability to control the shape and perimeter of various habitat patches. Contreras and Chung (2013) designed a computerized approach to optimize individual tree removal and produce site-specific thinning prescriptions that efficiently reduce crown fire potential. These types of heuristic applications have been well developed in the last 20 years for large landscapes dominated by even-aged forestry, but have not been applied to the group-selection layout problem. This is primarily because of the lack of foundational forest inventory and geospatial data at the levels of accuracy and detail needed to properly apply heuristic methods. These levels of accuracy and detail are beginning to become obtainable with the evolution of new remote sensing technologies, such as airborne lidar.

Airborne discrete-return lidar is an active remote sensing technology that provides high-resolution three-dimensional measurements in the form of point clouds that provide precise *x*, *y*, and *z* coordinates of intercepted objects (e.g., vegetation, coarse woody debris, ground) (Wing et al. 2012). The data have proven to be useful for prediction and characterization of many forest attributes with new forest-management-related applications currently increasing. Individual tree stem maps are one of the unique geospatial products that can be derived from airborne lidar data, significantly enhancing our understanding and ability to manage forest ecosystems (Kaartinen & Hyyppä 2008, Wang et al. 2008, Reitberger et al. 2009, Li et al. 2012, Jakubowski et al. 2013). The data provide sufficient detail to accurately locate and estimate heights of individual trees across forested landscapes. Identifying individual trees using airborne lidar data is currently an active area of research, with numerous methods being used and assessed. The accuracies of the various methods are dependent upon the quality of airborne lidar data, method(s) being used, forest type and structure (e.g., tree density), and tree crown form (Vauhkonen et al. 2011). In open forest stands with relatively even spacing, it is possible to generate highly accurate census stem maps (Vauhkonen et al. 2011). Individual stand census stem maps provide many new opportunities in forest management, including the ability to optimize treatment layouts.

This study seeks to capitalize on this opportunity by developing and applying a new method for implementing group-selection treatments using airborne lidar-derived census tree stem map data for an open forest stand using a heuristic decision technique. In summary, this study's goal is to develop and apply a heuristic for generating and assessing group-selection treatment options, based on a set of specific management goals, using a lidar-derived individual tree stem map. The heuristics selects from a set of better treatment solutions to implement in the field using GPS receivers.

Management and Policy Implications

Group-selection silviculture has many beneficial attributes and has increased in application of the past 30 years. It allows for creation of openings to allow regeneration of shade-intolerant species while maintaining structure within the stand and promoting structural heterogeneity. However, implementation is often subjective. The combination of scheduling algorithms and remote sensing technologies affords a novel method to develop a group-selection prescription. The use of lidar-derived stem maps allowed for efficient field implementation of a chosen solution.

Methods

Study Area

The study was conducted at Blacks Mountain Experimental Forest (BMEF) in northeastern California (Figure 1). The experimental forest (40°40′N, 10 121°10′W) is managed by the USDA Forest Service Pacific Southwest Research Station and is located approximately 35 km northeast of Mount Lassen Volcanic National Park. The elevation ranges from 1,700 m to 2,100 m, and stands are dominated by ponderosa pine (*Pinus ponderosa* Dougl. ex P. & C. Laws) with some white fir (*Abies concolor* [Gord. & Glend.] Lindl.) and incense-cedar (*Calocedrus decurrens* [Torr.] Florin) at higher elevations. At lower elevations, Jeffrey pine (*Pinus jeffreyi* [Grev. & Balf.]; Oliver 2000) can also be found in some stands. Classified as an interior ponderosa pine forest type (Forest Cover Type 237) (Eyre 1980), the 4,358-hectare forest has a wide range of stand conditions as a result of past research and management activities, as well as disturbance events (Ritchie et al. 2007). The 162-hectare stand employed in this study is located in the southwest portion of BMEF (Figure 1). It was thinned in 2005 to reduce the potential threat of high-severity wildfire. The prescription involved a thinning from below with whole-tree removal to reduce surface and ladder fuels. Prior to this treatment, the stand had a density of approximately 1,200 trees hectare^{-1} and basal area of 30 m^2 hectare^{-1}. The treatment produced a uniform stand of Jeffrey and ponderosa pine trees in open-canopy, free-to-grow, conditions. There was no favoring between the two species for the management goals. A variable-radius plot sample conducted in 2009 provided estimates of post-thinning mean tree diameter at breast height (dbh) of approximately 37 cm and a basal area of 11.7 m^2 hectare^{-1}. These stand conditions provided a unique opportunity to test the goals of this study because: (1) the open nature of the stand ensured the feasibility of deriving an accurate individual tree census stem map, and (2) it was a good candidate for a group-selection treatment to increase heterogeneity by creating additional age cohorts within the stand. As part of the experimental design of the study and to increase the understanding of the silvicultural treatment, the stand was partitioned into three separate units. Two approximately 61-hectare units within the stand were designated to receive contrasting group-selection treatments while still treating the same amount of area within each unit; one unit was to receive larger group-selection openings (i.e., 0.6–0.8 hectares) and one unit was to receive smaller group-selection openings (0.3–0.4 hectares) (Figure 1). The remaining approximately 40 hectares was to receive no treatment to provide a control and help with treatment comparisons in the future.

Airborne Lidar Data

Airborne lidar data (discrete-return) were acquired over the entire BMEF study area in late July 2015 using a Leica ALS50 Phase II laser system mounted on a fixed wing aircraft by Quantum Spatial Inc. The aircraft was flown at 900 m above ground level following topography. The data were acquired using an opposing flight line side-lap of 50 percent and a sensor scan angle 14 degrees from nadir. The on-ground laser-beam diameter was approximately 25 cm. An overall average point density of 13.83 points m^{-2} was obtained for the study area, with an average ground classified point density of 2.46 points m^{-2}. The average relative vertical accuracy for the acquisition was 0.036 m. The vendor post-processed the lidar data and developed a digital elevation model (DEM) from the ground classified points. The DEM was used to generate a height-normalized lidar point cloud by subtracting the individual lidar point elevation values (i.e., *z*-values) from the corresponding DEM elevation values in the identical location (i.e., identical *x*- and *y*- values). The height-normalized point cloud was then clipped out to the study area with a 20-m buffer. This study area height-normalized point cloud was then used to generate the individual tree census stem map.

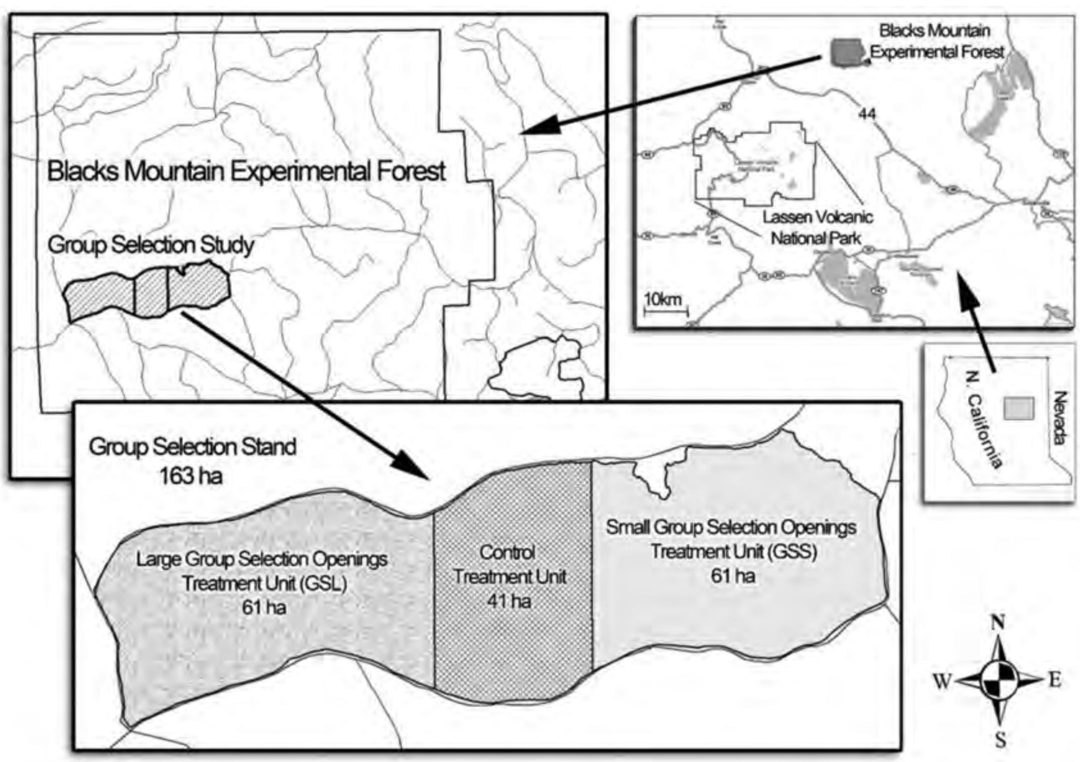

Figure 1. Location of Blacks Mountain Experimental Forest (BMEF) and the group-selection treatment study area.

Individual Tree Census Stem Map

A traditional individual tree identification procedure was applied to the study area's height-normalized lidar data to generate the initial individual tree stem map. In the first step of the individual tree identification procedure, a canopy surface model (CSM) was created using the height-normalized point cloud. CSMs can have various forms depending on how the surface is interpolated and smoothed. When the primary use for a CSM is to detect individual trees or snags, it is crucial that the CSM accurately represents individual trees by providing single height maxima for each tree while also following their crown profiles. In this study, the CSM was created using the "CanopyModel" command line utility processing program in the Fusion lidar software package (McGaughey 2012). CanopyModel creates an interpolated CSM using the lidar point cloud. The default setting assigns the elevation of the highest return within each grid cell to the grid cell center. The program provides additional smoothing of the generated surface using median or mean filters (McGaughey 2012). It is also capable of preserving local maxima in the surface while smoothing to force the surface to adhere to the tops of trees. This study used a cell size of 0.6 m^2, 3 × 3 median and 5 × 5 mean smoothing filters, and preservation of the local maxima (i.e., peaks switch) to create the CSM.

After the CSM was completed, the CSM was used to identify individual trees by locating individual tree tops within the CSM using the automated command line utility processing program "CanopyMaxima" in the Fusion lidar software package (McGaughey 2012). In the program, the location of individual trees is estimated by searching for local height maxima in the CSM using a variable-size window approach (Popescu and Wynne 2004). Initial values are seeded in every grid cell with a height value greater than the understory height threshold (1.5 m for this study) and allowed to climb in the direction of the steepest slope. When a seed reaches a position where all neighboring grid cells have lower height values, a local maximum is found. At each local maximum, the original x and y location of the highest point within the grid cell is designated as the tree's geospatial location, and the height value from the CSM as the tree's height. The program outputs a tree list with location coordinates, height values, and estimated crown width values in comma-separated file format.

Next, a manual interpretation-and-correction process was completed to remove errors associated with the initial individual tree census stem map (i.e., missing and fictional trees). To complete the manual interpretation process, the initial census stem map was input into the Fusion software's "lidar data viewer" (LDV). The LDV provides a three-dimensional (3D) visualization environment for the examination and measurement of spatially explicit lidar data subsets. In the LDV, the height-normalized lidar point cloud data and the individual tree census stem map data are viewable simultaneously. Lidar point cloud data are represented by individual colored shapes (e.g., dots) based on their location in 3D space. Individual tree data are represented as a colored wire mesh frame for each tree crown based on a tree's location, height, and crown width information. The LDV provided a unique manual interpretation and correction environment, where missing and fictional trees were added or removed accordingly. This process, which included two correction iterations, was completed in 4 days for the 163-hectare study area. The end result was a geospatial census stem map for the entire study area (Figure 2). A stem map accuracy assessment was completed in the field, where individual trees were identified and verified over approximately 25 percent of the stand surveyed to help determine the overall accuracy of the final stem map. The final stem map was input into ArcGIS and transformed into a set of nodes and arcs that were used to generate the geospatial data layers needed to implement the group-selection treatment heuristic and produce a solution. This included the conversion of the point data to polygons with a unique set of nodes and arcs for the data.

Heuristic Input Data Creation

In ArcGIS, the individual tree stem map point attribute data were linked to their respective treatment units. The dbh values were estimated for each tree point using local height-versus-dbh equations. The dbh distributions for each treatment unit were then generated to aid in the development of treatment objectives and goals (Figure 2). Cubic foot volume was estimated for each tree using a regional ponderosa pine volume equation (Wang 2017). The dbh and cubic foot volume values were also estimated for each tree 25 years in the future using a locally developed growth model. The growth model predicted dbh growth over 5-year intervals and was developed using BMEF tree data from stands with similar conditions that were re-measured at 5-year intervals over the past 20+ years.

Next, Thiessen polygons were generated within each treatment unit from the corresponding tree stem map point data. Aakala et al. (2013) used Thiessen polygons as a component of an intertree competition index for pine. We are using this method to identify the forest area associated with each tree in the stand. This process assigned each tree to its own individual Thiessen polygon, where each polygon area represents the area that is closer to its associated input tree point than to any other tree point (Figure 2). The coordinate geometry data was created for each polygon that developed a unique set of nodes and arcs for the polygons. Additionally, other attribute data were assigned to polygons based on the tree's characteristics. These included: (1) the current and 25-year dbh, height, cubic foot volume, and area (ha) associated with each tree's Thiessen polygon; (2) the arcs and arc lengths. The area for each tree's Thiessen polygon was calculated using the "calculate areas" tool in ArcGIS. The arcs, arc lengths, and associative tree IDs were generated, calculated, and assigned using the "clean (coverage)" tool in ArcGIS. Since all species were pine, there was no need to maintain the species identification. The adjacency list was generated using the "generate spatial weights matrix" and "convert spatial weights matrix to table" tools in ArcGIS. Once these geospatial data were generated, they were used as the foundational inputs in the heuristic.

Treatment and Heuristic Objectives

Before developing a heuristic, treatment goals and constraints need to be defined and an objective function formulated governing the candidate solution and selection process. The primary treatment goals for the two 61-ha units were to create contrasting opening sizes between the units while also treating the same area within each unit (approximately 16 percent of total area). In the larger group-selection opening treatment unit (GSL), eight openings of approximately 0.6 hectare and six openings of approximately 0.8 hectare were to be installed and treated in 2017 and 2042. In the smaller group-selection treatment unit (GSS), 16 openings of approximately 0.3

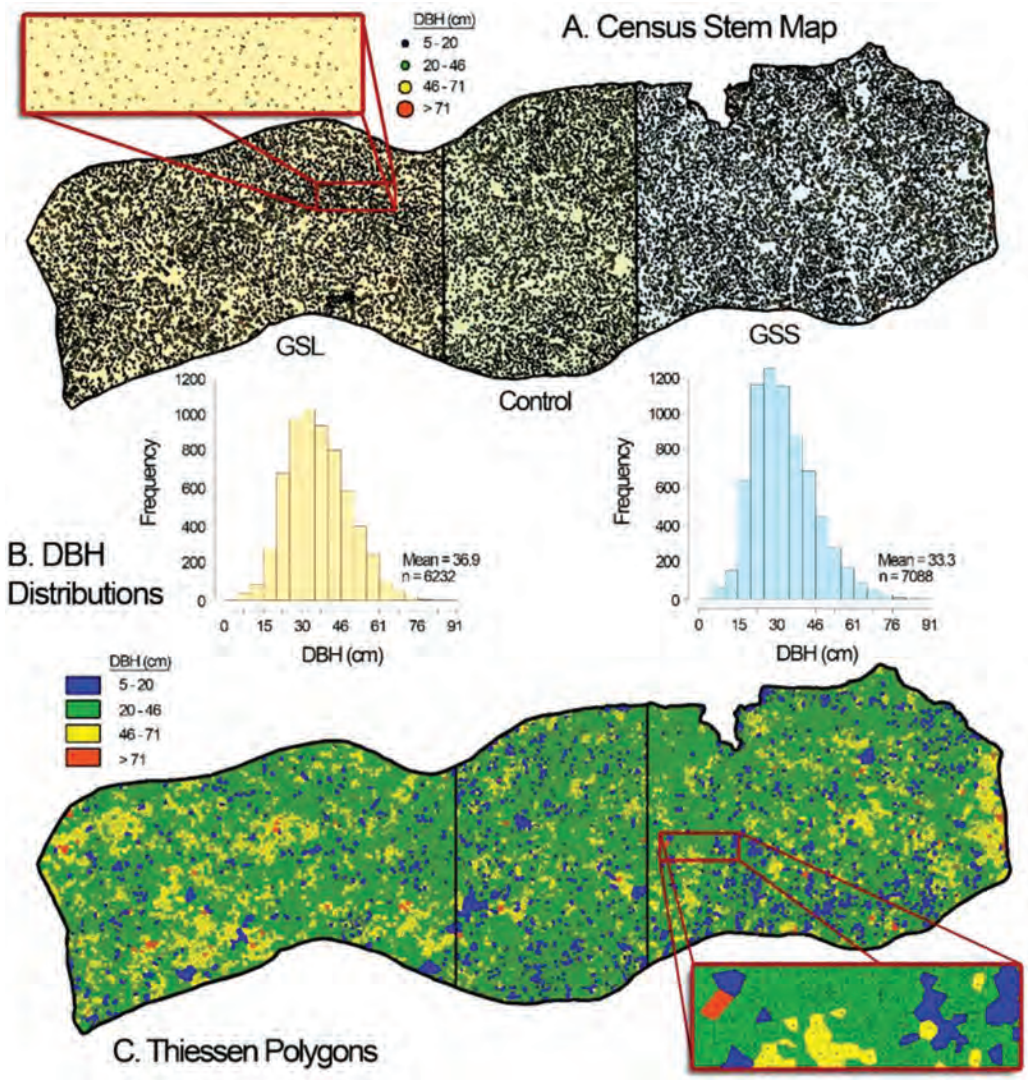

Figure 2. Depiction of group-selection stand census stem map data and derivatives. (A) Individual tree census stem map. (B) diameter at breast height (dbh) (cm) distributions for the treatment areas. (C) Individual tree Thiessen polygons derived from the census stem map colored by dbh classes. GSL: large group-selection openings treatment area; GSS: small group-selection openings treatment area.

hectare and 12 openings of approximately 0.4 hectare were to be installed and treated in 2017 and 2042. The treatment objectives were focused on implementing these group-selection treatments in a manner that balanced for multiple management goals over time. These goals were then translated into mathematical goals that could be integrated into a heuristic procedure. We realize that not all goals can be adequately represented mathematically, but in this case we were able to adequately transfer the landowner objectives into rules to guide the heuristic solution. The primary management goals and subsequent rules that governed the heuristic were as follows:

- Treat approximately 16 percent of the treatment units on each entry.
  - GSL: eight each of approximately 0.6-hectare openings and six each of approximately 0.8-hectare openings.
  - GSS: 16 each of approximately 0.3 hectare openings and 12 each of approximately 0.4-hectare openings.
  - Provide an incentive to select solutions with more area being treated.
- Increase structural complexity within the units.
  - Treatments were to target the removal of trees with dbhs between ±1 standard deviation from the mean dbh for each entry (entry 1: 20–46 cm; entry 2: 30–56 cm), but would also allow for approximately 10 percent of smaller and larger trees to be randomly selected for removal to broaden the candidate solution pool.
- Space the group-selection openings across the treatment areas.
  - No group-selection openings were allowed to be located within 80 m of each other in the GSL unit and 50 m in the GSS unit.
- Provide a stable flow of timber volume over two entries, 25 years apart.
  - Target total harvest volumes (cubic foot) that are near or greater than the mean total harvest volumes available for each entry.
    - Mean total harvest volume reference values for each entry determined from an initial exploratory analysis of 1,000 candidate solutions for each entry.

- Penalize solutions that are less than 5 percent of the mean total harvest volume reference value.
- Reduce positive influence of solutions with total harvest volume values greater than 5 percent of the mean total harvest volume reference value.

- Maximize group-selection opening edge.
  - Provide an incentive to choose solutions that provided more opening edge.
    - Reduce influence compared with total harvest volume and area.

Heuristic Design and Implementation

The primary goal of a heuristic is to search a problem's solution space and identify solutions that provide the best alternatives for meeting specific objectives. This study required development of a technique to generate and assess solutions. The algorithm uses a Monte Carlo method that selects polygons to join the solution. Monte Carlo has been validated against simpler problems using just the unit-exclusion for the green-up constraint that resulted in the best performance of the solutions between 86 and 96 percent of the optimal solution (Boston et al. 1999). The first step was to develop a method to generate candidate group-selection treatment solutions that adhered to the treatment objectives outlined in the previous section. The heuristic decision workflow is outlined in Figure 3. Solutions were built using a Monte Carlo random process with constraints (i.e., tree size, opening spacing, and size) to ensure the solutions adhered to the treatment objectives outlined in section 2.5 (Figure 3). The random nature of the candidate solution generation process provided the means to adequately search throughout the problem's solution space and identify better solutions. Individual trees were first randomly selected to build potential group openings, and then additional trees were randomly added to the openings until the opening reached the proper size (Figure 3). After all openings reached their respective area targets for the first entry (2017), the process was repeated for the second entry (2042) with trees harvested in the first entry unavailable for removal in the second entry. After a candidate solution was generated, it was assessed and ranked using an objective function with the following form:

$$\text{Maximize: } Z = \sum V_j - Vp_j - A_j + 0.65E_j \quad (1)$$

$$(1)\ \sum\sum \mathrm{Vol}_{ij} X_{ij} - V_j = 0 \quad (2)$$

$$(2)\ 1.05V_j - V_t - Vp_j \geq 0 \forall j \quad (3)$$

$$(3)\ 0.95V_j - V_t - Vp_j <= 0 \forall j \quad (4)$$

$$(4)\ \left(\sum \mathrm{Area}_{kj} X_{ij} - \mathrm{Areag}_j\right) / \mathrm{Areag}_j - A_j = 0 \forall j \quad (5)$$

$$(5)\ \left(\sum \mathrm{Edge}_{kj} X_{ij} - \mathrm{Edgeg}_j\right) / \mathrm{Edgeg}_j - E_j = 0 \forall j \quad (6)$$

where: X_{ij} = tree i treated in period j elements of {0,1}, decision variable; Vol_{ij} = volume from treating tree i in period j, a parameter; V_j = accounting variable for total volume in period j; Vp_j = penalty volume for period j; Area_{kj} = area of cluster k in period j; Areag_j = area goal in period j; A_j = accounting variable for area goal in period j; edge_{kj} = edge of cluster k in period j; Edgeg_j = edge goal in period j; E_j = accounting variable for edge goal in period j; and Vol_{mj}, Area_{mj}, and Edge_{mj} values were calculated from an initial exploratory analysis of 1,000 candidate solutions.

One thousand candidate solutions were initially generated, and the rounded mean values for treatment harvest volume, area, and edge from those solutions were used to bring the three objective function variables into a more common scale (Table 1). After inspection of the initial solutions, an additional weight reduction was administered to the edge variable (E_j) that is reflected in the value selected in the current model. The purpose was to decrease its influence on the objective function. This was done for two reasons: (1) it was decided that this variable was less important than the other variables, and (2) its higher range of variability required a reduction to bring the variable into a more consistent scale with the other two variables.

The stopping rule used for the heuristic was to terminate its exploration of the solution space after 500 consecutive solutions were found without improving one of the top three solutions. Treatment solutions were ranked based on their objective function values, and the top three solutions were retained for further visual inspection. In the final step, the three best solutions were visually inspected in ArcGIS, and one of the solutions was selected for implementation based on a visual inspection of the layout. This allowed for exploitation of the mathematical nature contained in the goals for this problem, but allowed the candidate solutions that are reviewed prior to their implementation. A level 1 validation approach was used in this model, with a well-known heuristic applied to a new problem; no additional validation was performed.

Field Implementation

After selecting a solution to implement, the next objective was to create an efficient method to mark the trees identified for removal in the field. Marking the trees was completed by loading two geospatial tree stem map layers onto two high-accuracy (i.e., ±2 m) handheld GPS units that use GPS and GLONASS global navigation satellite systems simultaneously. The first layer was the census tree stem map for the entire stand to be used for spatial orientation in the field, and the second layer comprised the removal-only tree stem map for each treatment unit used to identify removal trees in the field. Two crews of three field technicians were each given one GPS unit. One of the crew members navigated to and identified the trees slated for removal using the GPS unit; the other two crew members followed and marked the identified removal trees. The process was repeated until all the group-selection openings were marked. The time needed to complete the tree marking for each unit was recorded.

Results

We first evaluated the GSL and GSS treatments. Figure 4 provides frequency distributions for the three objective function variables, total number of trees selected, and objective function values from a random subset (n = 1,200) of all the candidate solutions that were assessed in the heuristic (GSL: n = 3,216; GSS: n = 2,996). Of the top three solutions identified by the heuristic, the final solutions selected for implementation in the GSL and GSS treatment units

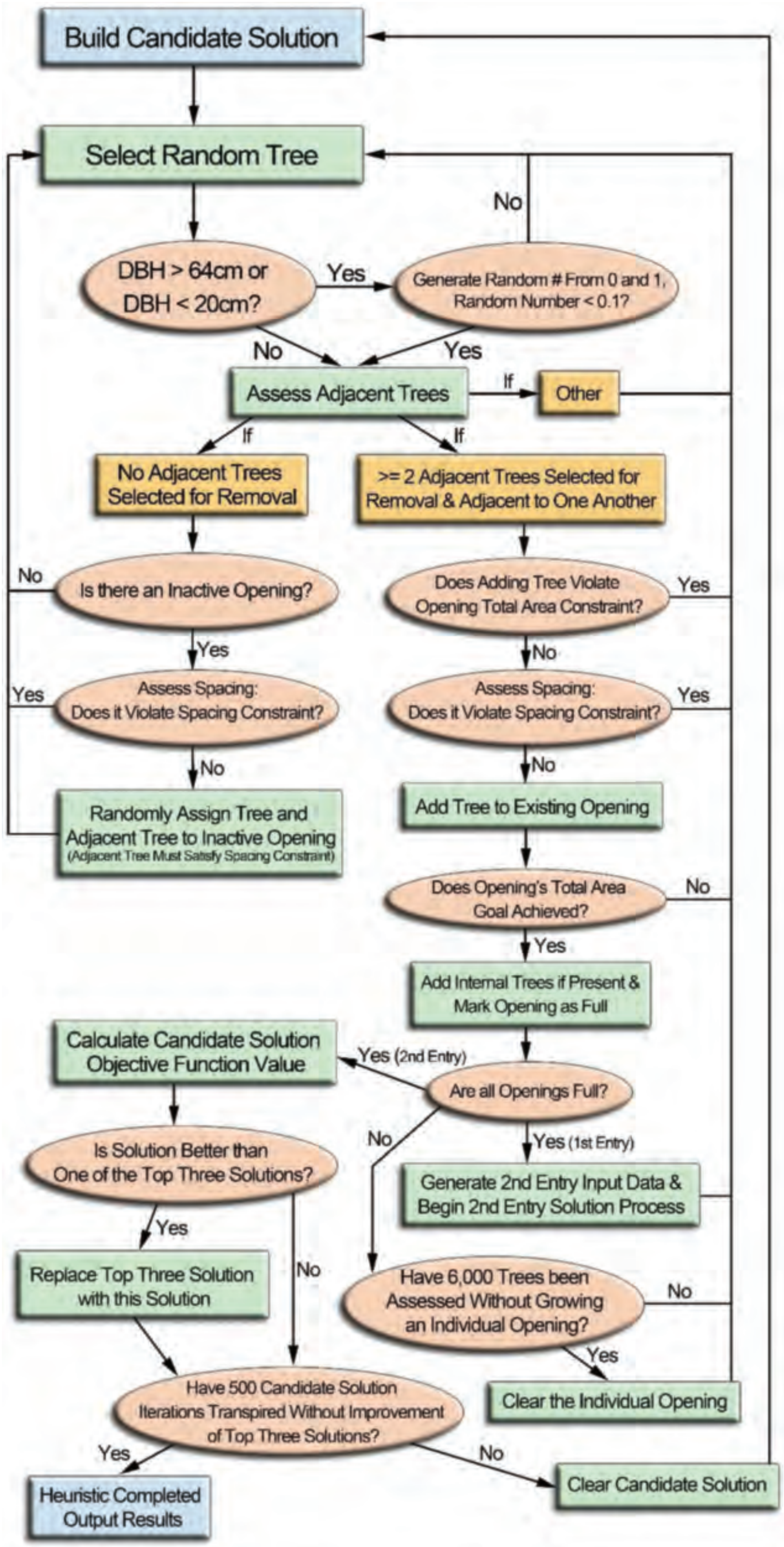

Figure 3. Group-selection treatment heuristic workflow.

produced total harvest volumes of 234 m^3 and 224 m^3 for the first entry, and 462 m^3 and 454 m^3 for the second entry respectively. Increases in second entry harvest volumes were directly related to tree growth and tree size availability. The total treated area for the two entries remained relatively stable over the two entries and between treatment stands (GSL: 10 hectares and 9.9 hectares; GSS: 10 hectares and 9.8 hectares). The total opening edge remained stable over the two entries, but the GSS treatment had a significantly higher amount of edge created, because more openings were created (GSL: 7,537 m and 7,345 m; GSS: 10,153 m and 10,034

Table 1. Objective function reference variable values used for the large and small group-selection treatments.

	Objective function reference values				
	Vol_m (cuft)	Vol_{m95} (cuft)	Vol_{m105} (cuft)	$Area_m$ (ha)	$Edge_m$ (m)
GSL treatment					
Entry 1	8,250	7,830	8,660	9.83	7,100
Entry 2	15,330	14,580	16,080	9.79	7,000
GSS treatment					
Entry 1	7,420	7,040	7,790	9.83	9,700
Entry 2	15,250	14,500	16,000	9.79	9,500

Note: Calculated from 1,000 candidate solutions. Vol_m: mean harvest volume; Vol_{m95}: 95 percent of mean harvest volume; Vol_{m105}: 105 percent of mean harvest volume; $Area_m$: mean treatment area; $Edge_m$: mean treatment edge.

m). The objective function values for the best-found solutions were about 31 percent greater for both treatment units than the mean objective function values from the respective candidate solutions, a proximate solution using a manual method for creating and assigning the groups to periods. For both treatment units, approximately 4 percent of the removal trees had dbhs less than the entry's minimum target dbh, and approximately 10 percent had dbhs greater than the entry's maximum dbh target. The best solutions for both GSL and GSS units are depicted in Figure 5.

Lidar-Derived Individual Tree Census Stem Map Accuracy

The overall individual tree census stem map used in the study had a very high accuracy (overall error rate: 0.09 percent). The field individual tree accuracy assessment surveyed approximately 25 percent of the unit areas spilt evenly between the two treatment units. A total of approximately 1,600 trees were surveyed on each of the treatment units. The manual inspection survey produced a total of two commission errors (0.06 percent) and one omission error (0.03 percent). Both commission errors were associated with forked top trees. The one omission error was associated with a tree that had its crown intermixing and overtopped by a larger tree. The stand conditions created by the 2005 thinning treatment resulted in a stand in which this type of situation was in effect nonexistent.

Heuristic Performance

The Monte Carlo heuristic developed in this study produced candidate solutions that met all treatment objectives (i.e., opening size and spacing, increased structural complexity, stable harvest volume). We have employed the validation procedure recommended by Bettinger et al. (2009) for a well-established heuristic, in this case a Monte Carlo integer programming problem that has being applied to new problem, but has had a full evaluation of the heuristics performed for a simpler problem (Boston and Bettinger 1999). Individual candidate solutions were generated in an average of 112 s (range: 85–208 s) for the GSL treatment unit, and 119 s (range: 82–218 s) for the GSS treatment unit. The total length of time to run the heuristic for the GSL treatment unit was 102.7 h, and 97.3 h for the GSS treatment unit.

Field Implementation

Marking of selected removal trees was completed over two days in June 2016 using two crews comprising three field technicians each. The GSL treatment unit was completed in 6.4 h, and the GSS treatment unit was completed in 8.1 h. The additional time needed to complete the GSS unit tree mark was directly related to the difference in the number of group-selection openings between the two treatment units. The total amount of time needed to mark the trees and group-selection boundaries was lower than the typically required time by an estimated 25 percent, based on discussions with the tree-marking crew.

Discussion

This study introduced a new method for developing and implementing group-selection treatments using airborne lidar-derived census stem map data in a heuristic environment for multiple management goals. The method successfully generated and assessed viable group-selection treatment solutions, which adequately searched throughout the problem's solution space to identify a set of better solutions for the specified treatment objectives. From this selected set, a solution was chosen to implement in the field. This required the development of a new tree-marking technique that used high-accuracy handheld GPS units to identify individual trees selected for removal. The method outlined in this study provides an improved and mathematically defendable technique for implementing group-selection treatments and also introduces a new application for geospatial stem map data.

A number of factors affected our ability to successfully generate, assess, and select solutions. The airborne lidar-derived geospatial census stem map provided the foundational data for the method. Thus, the accuracy of the stem map was paramount in the ability of the method to produce accurate and representative results. All of the components that make up the census stem map creation process can affect the accuracy of the stem map. The quality and point density of the airborne lidar data make up the first component. They are both paramount to the method's ability to generate a CSM that can be used to identify individual trees. If the lidar point vertical and horizontal accuracies are poor (e.g., >30 cm) the creation of a CSM that adequately represents individual tree crowns becomes more difficult. In addition, if the average lidar point densities are too low (<3 points m^{-2}), it becomes more difficult to identify and differentiate the individual tree crowns from the lidar point clouds. Both the lidar quality and density for this study were at the levels required to create a CSM that could be used to identify individual tree crowns (accuracy: 0.036 m; point density: 13.83 points m^{-2}). The CSM creation and individual tree identification methods form the next component of the census stem map creation process that affects stem map accuracy. CSM resolution (i.e., grid cell size), smoothing techniques and local peak preservation methods significantly impact the ability to identify individual trees tops from the CSM. There are also a number of parameters that govern the individual tree-identification process. Both the CSM and individual

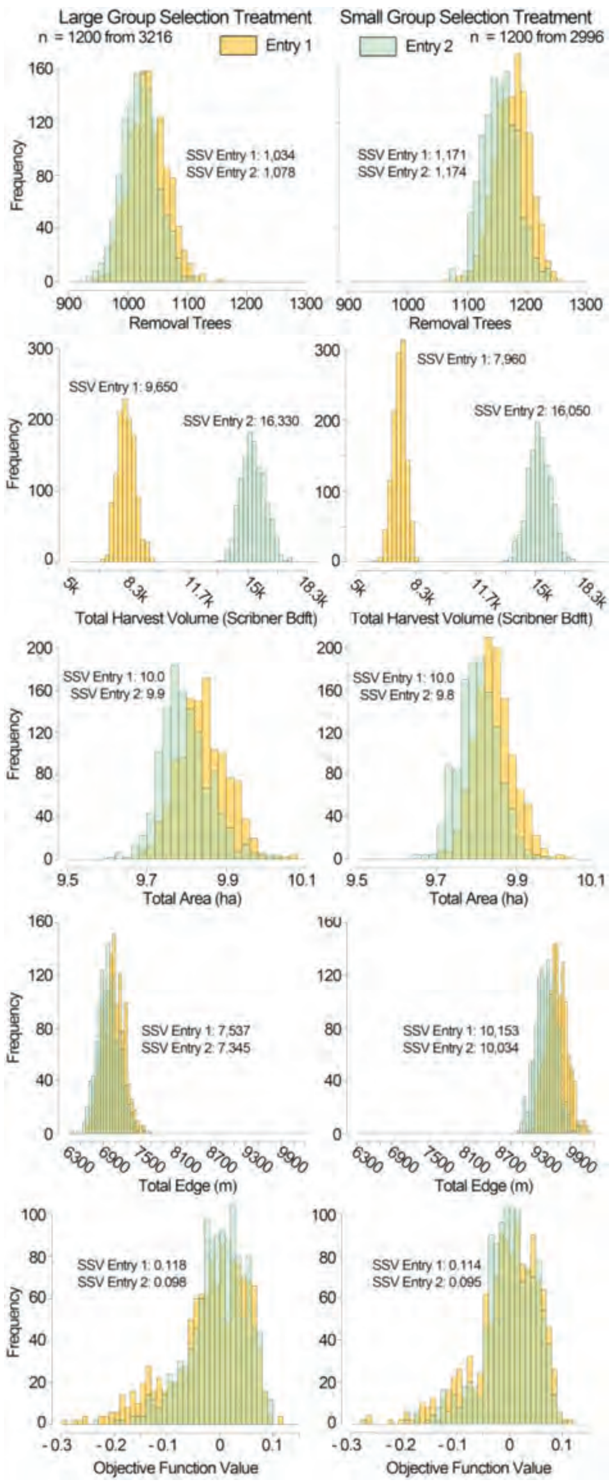

Figure 4. Frequency histograms for objective function values and candidate solution variables. Generated from 1,200 randomly selected candidate solutions (GSL: *n* = 3,215; GSS: *n* = 2,996) for both the large and small group-selection treatments. SSV: selected solution value.

tree identification parameters typically require a manual adjustment and honing process to produce accurate stem maps. The first goal of the process is to generate a CSM that adheres to the individual tree crowns without creating fictional tree tops or missing tree tops that are intermixed with neighboring tree crowns. The second goal is to identify the individual tree tops on the CSM. The method used in this study successfully identified all but 32 trees based on the manual inspection and correction procedure.

The most crucial component of the census stem-map creation process was the manual stem map inspection and correction procedure. The procedure was crucial to help ensure there were no fictional or missing trees. The process was relatively simple to implement using the Fusion LDV. Its unique ability to simultaneously visualize the point cloud with the tree stem map data in 3D provided the capability to manually add and remove trees as necessary. In all, there were 164 fictional trees removed and 32 trees added during the manual inspection and correction process. The fictional trees were most often found on the edges of larger tree crowns, which was an artifact of the CSM creation process (e.g., utilizing the "peaks" switch in the fusion "CanopyModel" program). The stem map created after the manual creation process served as the final tree stem map and was highly accurate based on the field individual tree assessment survey (i.e., error rate of 0.09 percent). It is important to note that the stand used in this study is very open with low structural complexity and comprises ponderosa and Jeffery pine, which were treated identically silviculturally. These traits made the ability to generate an accurate census stem map ideal. When generating stem maps in more structurally complex, closed canopy, and species-rich stands it will be more difficult to generate accurate census tree stem maps using the method outlined in this study. That said, the concepts presented in this study might also be feasible to implement with coarser-scale geospatial tree data. However, the identification of the points from the dominate trees may be sufficient to implement a group-selection treatment. For example, it might be possible to use raster-based geospatial tree data derived from airborne lidar (e.g., canopy cover, basal area, volume, biomass, tree density, etc.) at meaningful spatial resolutions (e.g., <30 m × 30 m) in a heuristic environment to develop more optimal treatment solutions for specific management goals.

The techniques for deriving individual tree heights, dbhs, and volumes also likely affected the overall accuracy of the method. Height values were estimated from the lidar CSM-based individual tree identification procedure. There is a known slightly negative bias associated with tree heights using this procedure, which could have been transferred into the dbh and volume predictions (Gatziolis et al. 2012). The negative height bias is typically within the field tree height measurement error, so it is unlikely it would have changed the results of this study. The dbh, volume and growth models used to predict both the current and future tree dbhs and volumes likely introduced additional variability into the method. It is crucial to use the best available models for prediction of dbh and volume to reduce these sources of variability.

The heuristic's candidate solution creation process was another factor that affected the overall results of the method. The heuristic rules and constraints that were constructed and applied impacted how the candidate solutions were generated and ultimately selected. A trial-and-error process was used to determine the best technique(s) to apply the rules and constraints to meet the treatment objectives. This step was crucial to ensure candidate solutions were truly representative of treatment objectives and provided viable solutions. The treatment opening spacing constraint was the most difficult constraint to define. If the opening spacing requirement was too large (e.g., GSL: >120 m; GSS: >80 m) the development of feasible solutions became much more limited or impossible and caused significant increases in the heuristic's run time. On the other hand, if the spacing

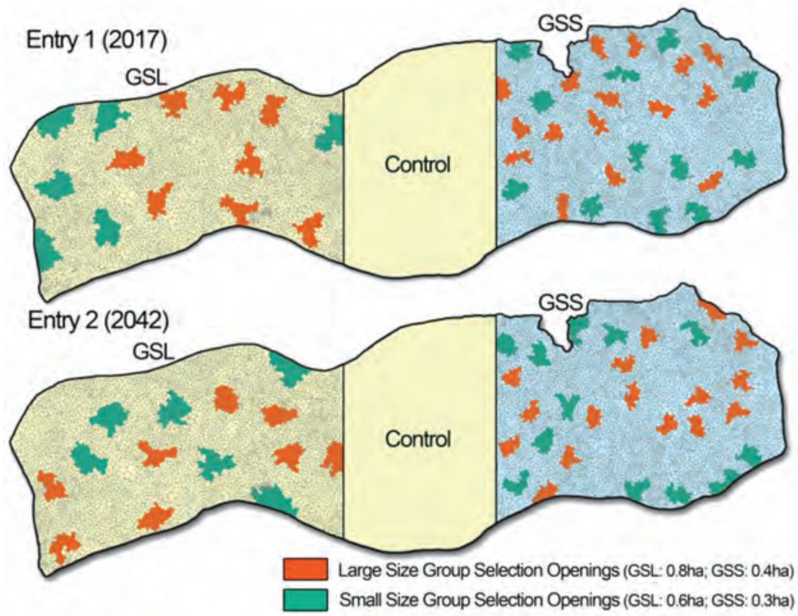

Figure 5. Depiction of the most optimal group-selection treatment solution identified by the heuristic. GSL: large group-selection treatment; GSS: small group-selection treatment.

requirement was too small, it became possible to generate solutions that produced openings that were not adequately spread out over the entire treatment area. The inclusion of the large and small tree constraint (i.e., 10 percent chance of including large and small trees in the solution) helped to broaden the candidate solution pool.

The objective function determines how candidate solutions are ranked and ultimately selected by the heuristic. The objective function used in this study was relatively simple with three variables. Weighting these variables changes their respective influence, and thus the decision of each variables importance is required to make a meaningful objective function. These decisions are typically made during the formulation of the treatment objectives. In this study, it was decided that the total treatment edge variable (E_j) was not as important as the total volume and area treated variables, so it was reduced. This decision was primarily based on the current open nature of the stand. The volume penalty reduced the influence of candidate solutions with total harvest volumes $<Vol_{m95}$ or $>Vol_{m105}$. The penalty adversely affected candidate solutions with harvest volumes $<Vol_{m95}$ more significantly than candidate solutions with total harvest volumes $>Vol_{m105}$. For candidate solutions with total harvest volumes $>Vol_{m105}$, the penalty reduced the influence of the volume variable while also allowing it to slightly improve the objective function. Since this was an early study to use geospatial stem map data in this type of heuristic application, there are likely a number of opportunities available to improve the method. The census stem-map creation process could be improved. The method required a large time investment to generate the highly accurate stem map, primarily because of the manual inspection and correction procedure. With the advent of new airborne lidar-based individual tree identification methods that provide more accurate tree-stem-map data, it might become possible to reduce or eliminate the manual inspection and correction process altogether. In addition, as airborne lidar data quality and accuracy continue to improve, and point densities increase, the ability to identify individual trees and derive their true heights should also improve. Both would enhance the overall accuracy of this study's method.

The technique used to generate candidate solutions can be made more efficient. An approach that builds the treatment openings outward from random seed trees warrants further investigation, because it could reduce the time required to formulate potential solutions. This study's candidate solution-creation process also required a method to become freed if a potential opening was unable to grow to the necessary size because of the adjacency spacing constraints (i.e., the opening would not fit in that location because of neighboring openings). A simple maximum iteration threshold constraint was used to determine whether any of the openings needed to be moved. Creating individual group-selection openings sequentially instead of simultaneously might produce candidate solutions more efficiently, or initial seed trees could be tested with larger adjacency distance requirements before becoming potential treatment opening starting-points.

The treatment objectives used in this study were relatively simple. Including additional treatment objectives, such as minimizing impacts from harvesting equipment (e.g., minimizing distance to existing skid trails and landings), promoting or maintaining wildlife habitat, and reducing fire behavior, all warrant exploration. Including these types of objectives will require additional attributes to be added to the stem map data, as well as development of new solution creation and assessment techniques. Individual tree characteristics such as tree crown health (e.g., live, dead, or dying) and wood quality are also starting to be explored using remote sensing data (Van Leeuwen et al. 2011, Wing et al. 2015). The inclusion of these attributes would likely improve the ability to develop more optimal forest management and planning strategies that balance for multiple goals overtime.

The scenario presented in this study assessed two treatment entry periods. The inclusion of additional treatment entries is possible using the methods outlined in this study, but it was deemed inappropriate for the following reasons. First, the management plan for the study area requires group-selection treatments to continue in the treatment units at the same periodicity, with trees planted in the initially created openings (2017) becoming available for removal in the third treatment (2067) onward. Given these trees will become potential removal trees in the third entry, it is difficult to know what the true stem map will be for the third treatment making the extension of the current heuristic inappropriate. Second, the continual advancement of remote sensing technologies will likely produce the ability to generate a census stem map with additional information in the future, which could improve the results of the heuristic for the third treatment entry. Lastly, there is a known temporal propagation of errors in dbh and volume predictions stemming from growth models. These errors would reduce the accuracy of the candidate solution creation and selection process. For these reasons, it was decided that it would be more appropriate to develop the third and fourth entry treatment solutions just before the third entry. The targeted dbh ranges will also require adjustment for future entries as the dbh distributions change overtime.

The field implementation of the selected solution was relatively simple and efficient. The high-accuracy GPS units were a key component to successful implementation. Navigating to individual removal trees using the GPS unit was a relatively simple process. Average GPS accuracies remained in the 0.5–3 m range throughout the marking process, and the ability to visually observe the localized stem map tree arrangements on the GPS unit helped with orientation and individual tree identification. The stand conditions (i.e., open canopy, 22 percent canopy cover, and relatively flat terrain) were ideal for accurate GPS navigation in a forested environment. GPS accuracy would not be as high in stands with denser canopy cover and more extreme topography. Thus, the method might not work as well in these situations. The time it took to complete the tree mark in the field was more efficient than a traditional group-selection tree mark.

Conclusion

This study highlights an early attempt to integrate airborne lidar-derived geospatial stem map data in a heuristic environment to develop and identify good solutions that are easily implemented for group-selection silvicultural treatments for multiple management goals. We were able to successfully develop and implement new methods to generate, assess, and select more optimal group-selection treatment solutions using the geospatial stem map data. We also created a reasonably efficient method for implementing the treatment solutions in the field. The methods presented in this study provided many improvements over current group-selection treatment implementation methods.

Given this was the first attempt to accomplish this study's goals, there are likely to be improvements available. Increases in candidate solution development efficiency and the addition of more complex management and treatment goals would likely enhance the utility of the method. It is also important to note that the stand conditions for this study were ideal for testing and accomplishing the study's goals. In stands with more structural complexity and higher canopy cover, adjustments to these procedures will be necessary. The rapid advancement of remote sensing based applications in forest ecology and management is undeniable. The geospatial products derived from these technologies, such as airborne lidar, provide levels of detail over broad spatial scales that have never previously been available and open the door to many new opportunities in forest management. As these remote sensing techniques become better developed, they may be applicable to a wider range of ecosystems with more complex stand structures. This study highlighted one of these new applications.

Literature Cited

Aakala, T., S. Fraver, A.W. D'Amato, and B.J. Palik. 2013. Influence of competition and age on tree growth in structurally complex old-growth forests in northern Minnesota, USA. *Forest Ecol. Manag.* 308:128–135.

Bettinger, P., J. Sessions, and K. Boston. 1997. Using tabu search to schedule timber harvests subject to spatial wildlife goals for big game. *Ecol. Modell.* 94(2–3):111–123.

Bettinger, P., J. Sessions, and K. Boston. 2009. A review of the status and use of validation procedures for heuristics used in forest planning. *Math. Comput. For. Nat. Res. Sci*. 1(1):26–37.

Bettinger, P., K. Boston, and J. Sessions. 1999. Combinatorial optimization of elk habitat effectiveness and timber harvest volume. *Environ. Model. Assess.* 4(2):143–153.

Boston, K., and P. Bettinger. 1999. An analysis of Monte Carlo integer programming, simulated annealing, and tabu search heuristics for solving spatial harvest scheduling problems. *For. Sci.* 45(2):292–301.

Boston, K., and J. Sessions. 2006. Development of a spatial harvest scheduling system to promote the conservation between indigenous and exotic forests. *Int. Forest Rev.* 8(3):297–306.

Coates, K.D. 2000. Conifer seedling response to northern temperate forest gaps. *Forest Ecol. Manag.* 127:249–269.

Contreras, M.A., and W. Chung. 2013. Developing a computerized approach for optimizing individual tree removal to efficiently reduce crown fire potential. *Forest Ecol. Manag.* 289:219–233.

Eyre, F.H.. 1980. *Forest cover types of the United States and Canada*. Society of American Foresters, Washington, DC.

Fiske, J.N., S.J. Husari, T. Ratcliff, R.R. Rogers, and M.T. Smith. 1992. *Effects of a group selection strategy for the Sierra Nevada mixed conifer. Unpublished executive summary of regional ad hoc team.* San Francisco, CA. 1–3 p.

Gatziolis, D., J.S. Fried, and V.S. Monleon. 2012. Challenges to estimating tree height via LiDAR in closed-canopy forests: A parable from Western Oregon. *For. Sci.* 56(2):139–155.

Jakubowski, M.J., W. Li, Q. Guo, and M. Kelly. 2013. Delineating individual trees from lidar data: A comparison of vector- and raster-based segmentation approaches. *Remote Sens.* (5):4163–4186.

Kaartinen, H., and J. Hyyppä. 2008. *EuroSDR/ISPRS Commission II project: "Tree Extraction"—final report*. Official publication no. 53: EuroSDR. Frankfurt am Main, Germany. 60 p.

Lahde, E., O. Laiho, and Y. Norokorpi. 1999. Diversity-oriented silviculture in the Boreal Zone of Europe. *Forest Ecol. Manag.* 188:223–243.

Li, W., Q. Guo, M. Jakubowski, and M. Kelly. 2012. A new method for segmenting individual trees from the lidar point cloud. *Photogramm Eng. Remote Sensing* 78(1):75–84.

McDonald, P.M., and C.S. Abbott. 1994. *Seedfall, regeneration, and seedling development in group- selection openings.* USDA Forest Service, Research Paper. PSW-RP-220, Pacific Southwest Research Station, Albany, CA. 13 p.

McDonald, P.M., G. Fiddler, M. Ritchie, and P. Anderson. 2009. Naturally seeded versus planted ponderosa pine seedlings in group-selection openings. *West J. Appl. For.* 24(1):48–54.

McGaughey, R.J. 2012. *FUSION/LDV: Software for LiDAR data analysis and visualization—V3.10.* USDA Forest Service. USDA Forest Service, Pacific Northwest Research Station, Portland, OR. 168 p.

Moghaddas, J.J., B.M. Collins, K. Menning, E.E.Y. Moghaddas, and S.L. Stephens. 2010. Fuel treatment effects on modeled landscape level fire behavior in the northern Sierra Nevada. *Can. J. For. Res.* 40:1751–1765.

Oliver, W.W. 2000. *Ecological research at Blacks Mountain Experimental Forest in northeastern California.* USDA Forest Service General Technical Report PSW-GTR-179, Pacific Southwest Research Station, Albany, CA.

Popescu, S.C., and R.H. Wynne. 2004. Seeing the trees in the forest: Using Lidar and multispectral data fusion with local filtering and variable window size for estimating tree height. *Photogramm Eng. Remote Sensing* 70(5):589–604.

Reitberger, J., C.L. Schörr, P. Krzystek, and U. Stilla. 2009. 3D segmentation of single trees exploiting full waveform LIDAR data. *J. Photogramm. Remote Sens.* 64:561–574

Ritchie, M.W., C.N. Skinner, and T.A. Hamilton. 2007. Probability of wildfire-induced tree mortality in an interior pine forest: Effects of thinning and prescribed fire. *Forest Ecol. Manag.* 247:200–208.

Shlisky, A., J. Battles, R. Barrett, R. Heald, and B. Allen-Diaz. 1999. The effects of forest management on plant species diversity in the mixed conifer forests of the Sierra Nevada. Paper presented at Blodgett Forest Symposium, February 26–28, Georgetown, CA, 54–55.

Schultz, J.-P. 1999. Close-to-nature silviculture: Is this concept compatible with species diversity? *Forestry* 72(4):359–366.

Stephens, S.L., D.J. Dulitz, and R.E. Martin. 1999. Giant sequoia regeneration in group selection openings in the southern Sierra Nevada. *Forest Ecol. Manag.* 120:89–95.

Storer, A.J., D.L. Wood, T.R. Gordon, and W.J. Libby. 2001. Restoring native Monterey pine forests. *J. For.* 99(5):14–18.

Tóth, S.F., and M.E. McDill. 2008. Promoting large, compact mature forest patches in harvest scheduling models. *Environ. Model Assess.* 13(1):1–15.

Van Leeuwen, M., T. Hilker, N.C. Coops, G. Frazer, M.A. Wulder, G.J. Newnham, and D.S. Culvenor. 2011. Assessment of standing wood and fiber quality using ground and airborne laser scanning: A review. *Forest Ecol. Manag.* 261:1467–1478.

Vauhkonen, J., L. Ene, S. Gupta, J. Heinzel, J. Holmgren, J. Pitkänen, S. Solberg, Y. Wang, H. Weinacker, K.M. Hauglin, V. Lien, P. Packalén, T. Gobakken, B. Koch, E. Næsset, T. Tokola, and M. Maltamo. 2011. Comparative testing of single-tree detection algorithms under different types of forests. *Forestry* 85(1):27–40.

Wang, Y., H. Weinacker, B. Koch, and K. Sterenczak. 2008. LIDAR point cloud based fully automatic 3D single tree modelling in forest and evaluations of the procedure. *Int. Arch. Photogramm. Remote Sens. Spat. Inf. Sci.* 37(Part B6b):45–51.

Wang, Y. 2017. *National Volume Estimator Library—Volume Estimator Volume Equations.* USDA Forest Service, Forest Management Service Center, Ft. Collins, CO. Available at: www.fs.fed.us/fmsc/measure/volume/nvel/index.php.

Weatherspoon, C.P., and C.N. Skinner. 1996. *Landscape-level strategies for forest fuel management. Sierra Nevada Ecosystem Project, Final report to Congress, II: Assessments and scientific basis for management options.* Wildland Resources Center Rep. 37, Centers for Water and Wildland Resources, University of California, Davis, CA. 1471–1492 p.

Wing, B.M., M.W. Ritchie, K. Boston, W.B. Cohen, A. Gitelman, and M.J. Olsen. 2012. Prediction of understory vegetation cover with airborne lidar in an interior ponderosa pine forest. *Remote Sens. Environ.* 124:730–741.

Wing, B.M., M.W. Ritchie, K. Boston, W.B. Cohen, and M.J. Olsen. 2015. Individual snag detection using neighborhood attribute filtered airborne lidar data. *Remote Sens. Environ.* 163:165–179.

York, R.A., J.J. Battles, and R.C. heald. 2003. Edge effects in mixed conifer group selection openings: Tree height response to resource gradients. *Forest Ecol. Manag.* 179:107–121.